The American Journal of Human Genetics, Volume *93*

Supplemental Data

Mutations in *KARS*, Encoding Lysyl-tRNA Synthetase, Cause Autosomal-Recessive Nonsyndromic Hearing Impairment DFNB89

Regie Lyn Santos-Cortez, Kwanghyuk Lee, Zahid Azeem, Patrick J. Antonellis, Lana M. Pollock, Saadullah Khan, Irfanullah, Paula B. Andrade-Elizondo, Ilene Chiu, Mark D. Adams, Sulman Basit, Joshua D. Smith, University of Washington Center for Mendelian Genomics, Deborah A. Nickerson, Brian M. McDermott Jr., Wasim Ahmad, and Suzanne M. Leal

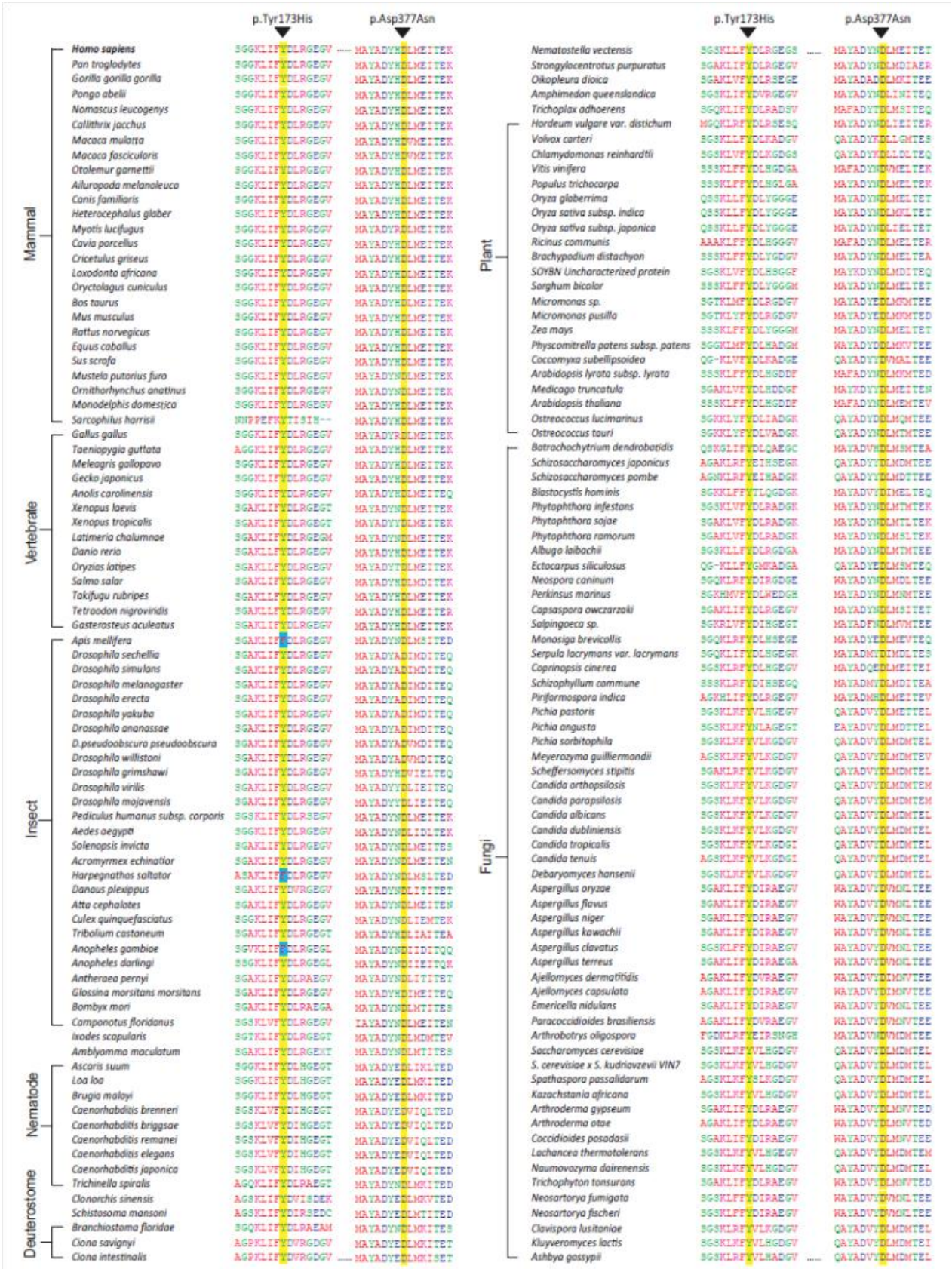
p.Tyr173His
p.Asp377Asn
Mammal
Homo sapiens
Pan troglodytes
Gorilla gorilla gorilla
Pongo abelii
Nomascus leucogenys
Callithrix jacchus
Macaca mulatta
Macaca fascicularis
Otolemur garnettii
Ailuropoda melanoleuca
Canis familiaris
Heterocephalus glaber
Myotis lucifugus
Cavia porcellus
Cricetulus griseus
Loxodonta africana
Oryctolagus cuniculus
Bos taurus
Mus musculus
Rattus norvegicus
Equus caballus
Sus scrofa
Mustela putorius furo
Ornithorhynchus anatinus
Monodelphis domestica
Sarcophilus harrisii
Vertebrate
Gallus gallus
Taeniopygia guttata
Meleagris gallopavo
Gecko japonicus
Anolis carolinensis
Xenopus laevis
Xenopus tropicalis
Latimeria chalumnae
Danio rerio
Oryzias latipes
Salmo salar
Takifugu rubripes
Tetraodon nigroviridis
Gasterosteus aculeatus
Insect
Apis mellifera
Drosophila sechellia
Drosophila simulans
Drosophila melanogaster
Drosophila erecta
Drosophila yakuba
Drosophila ananassae
D.pseudoobscura pseudoobscura
Drosophila willistoni
Drosophila grimshawi
Drosophila virilis
Drosophila mojavensis
Pediculus humanus subsp. corporis
Aedes aegypti
Solenopsis invicta
Acromyrmex echinatior
Harpegnathos saltator
Danaus plexippus
Atta cephalotes
Culex quinquefasciatus
Tribolium castaneum
Anopheles gambiae
Anopheles darlingi
Antheraea pernyi
Glossina morsitans morsitans
Bombyx mori
Camponotus floridanus
Nematode
Ascaris suum
Loa loa
Brugia malayi
Caenorhabditis brenneri
Caenorhabditis briggsae
Caenorhabditis remanei
Caenorhabditis elegans
Caenorhabditis japonica
Trichinella spiralis
Deuterostome
Clonorchis sinensis
Schistosoma mansoni
Branchiostoma floridae
Ciona savignyi
Ciona intestinalis
Plant
Nematostella vectensis
Strongylocentrotus purpuratus
Oikopleura dioica
Amphimedon queenslandica
Trichoplax adhaerens
Hordeum vulgare var. distichum
Volvox carteri
Chlamydomonas reinhardtii
Vitis vinifera
Populus trichocarpa
Oryza glaberrima
Oryza sativa subsp. indica
Oryza sativa subsp. japonica
Ricinus communis
Brachypodium distachyon
SOYBN Uncharacterized protein
Sorghum bicolor
Micromonas sp.
Micromonas pusilla
Zea mays
Physcomitrella patens subsp. patens
Coccomyxa subellipsoidea
Arabidopsis lyrata subsp. lyrata
Medicago truncatula
Arabidopsis thaliana
Ostreococcus lucimarinus
Ostreococcus tauri
Fungi
Batrachochytrium dendrobatidis
Schizosaccharomyces japonicus
Schizosaccharomyces pombe
Blastocystis hominis
Phytophthora infestans
Phytophthora sojae
Phytophthora ramorum
Albugo laibachii
Ectocarpus siliculosus
Neospora caninum
Perkinsus marinus
Capsaspora owczarzaki
Salpingoeca sp.
Monosiga brevicollis
Serpula lacrymans var. lacrymans
Coprinopsis cinerea
Schizophyllum commune
Piriformospora indica
Pichia pastoris
Pichia angusta
Pichia sorbitophila
Meyerozyma guilliermondii
Scheffersomyces stipitis
Candida orthopsilosis
Candida parapsilosis
Candida albicans
Candida dubliniensis
Candida tropicalis
Candida tenuis
Debaryomyces hansenii
Aspergillus oryzae
Aspergillus flavus
Aspergillus niger
Aspergillus kawachii
Aspergillus clavatus
Aspergillus terreus
Ajellomyces dermatitidis
Ajellomyces capsulata
Emericella nidulans
Paracoccidioides brasiliensis
Arthrobotrys oligospora
Saccharomyces cerevisiae
S. cerevisiae x S. kudriavzevii VIN7
Spathaspora passalidarum
Kazachstania africana
Arthroderma gypseum
Arthroderma otae
Coccidioides posadasii
Lachancea thermotolerans
Naumovozyma dairenensis
Trichophyton tonsurans
Neosartorya fumigata
Neosartorya fischeri
Clavispora lusitaniae
Kluyveromyces lactis
Ashbya gossypii

Figure S1. Multiple-Sequence Alignment for KARS and Similar Proteins

Aligned sequences are from 165 non-human species, including 8 primates, 14 placental mammals, 3 non-placental mammals, 3 avian, 2 reptiles, 2 amphibians, 7 bony fish, 27 insects, 2 arachnids, 9 roundworms, 2 flatworms, 8 water animals, 22 plants, 44 fungi and 12 other eukaryotes. Protein sequences were derived from the UniProtKB database using blastp and aligned using ClustalW2. For the human sequence, residues 166-180 and 370-384 from KARS (NP_001123561) are shown. The tyrosine residue at position 173 is highly conserved, and is replaced by a phenylalanine in only 3 of 165 proteins from non-human species (highlighted in cyan), namely *Harpegnathos saltator* (Jerdon's jumping ant), *Apis mellifera* (honeybee) and *Anopheles gambiae* (mosquito). The aspartic acid residue at position 377 (blue letters highlighted in yellow) is identical in all aligned sequences.

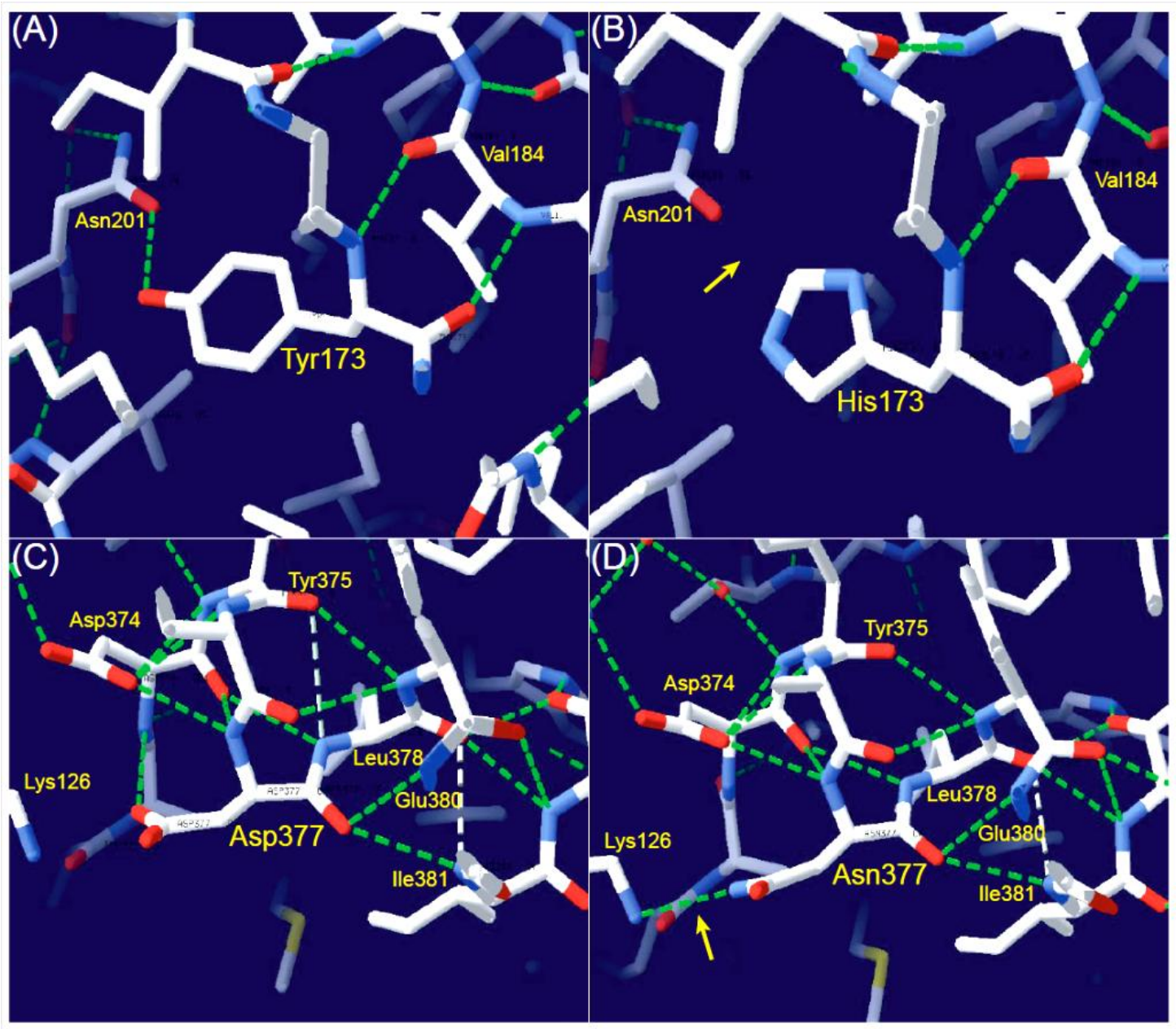

Figure S2. Structural Modeling for Altered KARS

H-bonds are shown as green dotted lines.

(A) Wild-type KARS with tyrosine at position 173.

(B) Altered KARS with histidine at position 173. Yellow arrow indicates loss of an H-bond between β-strand 2 and α-helix 3.

(C) Wild-type KARS with aspartic acid at position 377.

(D) Altered KARS with asparagine at position 377. Yellow arrow points to a gained H-bond between interacting KARS monomers. Additionally an H-bond between asparagine residues at positions 374 and 377 is lost, possibly resulting in loss of α-helix 9.

Table S1. ABR Findings in Individuals with *KARS* Mutations

Individual ID	dB	Side	Latency Wave I (ms)	Latency Wave III (ms)	Latency Wave V (ms)	Inter-peak I-III	Inter-peak III-V	Inter-peak I-V
4406 IV-2	100	Right	1.30	3.65	5.55	2.35	1.90	4.25
		Left	1.10	3.55	5.05	2.45	1.50	3.95
	90	Right	2.85	4.95	7.00	2.10	2.05	4.15
		Left	1.90	4.00	6.05	2.10	2.05	4.15
	80	Right	--	3.35	--	--	--	--
		Left	--	--	5.95	--	--	--
4406 IV-7 [a]	100	Right	1.00	3.60	5.65	2.60	2.05	4.65
		Left	1.31	4.65	6.85	3.34	2.20	5.54
	90	Right	--	3.40	5.05	--	1.65	--
		Left	--	3.10	5.90	--	2.80	--
	80	Right	--	5.23	--	--	--	--
		Left	--	--	--	--	--	--

[a] For individual IV-7 the compliance peak for the tympanogram on the left ear was absent (type B ear), indicating possible middle ear effusion or otitis media at the time of testing.

Table S2. Interexonic Primer Pairs for Zebrafish and Mouse *Kars* Gene

Exon	Forward	Reverse
zf_Kars_1	CAGAATATGCCAACTGCAAGCGC	CCATGACCTGCAGCTTGACTCC
zf_Kars_2	CCTGATCCCTGGTGGCGCAGT	AGCTCTTGGGTCATGCTGATTCG
zf_Kars_3	GGAGGTGAAGTGCATCAACCCAA	CCCTCTGCAGGTGCAGCTGGT
Mus_Kars_1	TCAGAGGGAACTTCGACTGGGC	GTTGGCCATGACTTGTAACTTGAC
Mus_Kars_2	GAGACATAATTGGAGTTGAGGGCA	TGCATAGGCCATGTAGAACTCACA
Mus_Kars_3	TCAGCATGGTAGAAGAGCTTGAGA	ATCGGTGAGAAACATGGTGAGCC